Summer 2009

Analysis of organic aerosol in Houston, TX, through aerosol mass spectrometry and proton nuclear magnetic resonance spectroscopy

Meredith J. Cleveland
University of New Hampshire, Durham

ANALYSIS OF ORGANIC AEROSOL IN HOUSTON, TX, THROUGH AEROSOL MASS SPECTROMETRY AND PROTON NUCLEAR MAGNETIC RESONANCE SPECTROSCOPY

BY

Meredith J. Cleveland
Bachelor of Science, University of Virginia, 2007

THESIS

Submitted to the University of New Hampshire
in Partial Fulfillment of
the Requirements for the Degree of

Master of Science
in
Earth Sciences

August 2009

This thesis has been examined and approved.

Thesis Director, Robert J. Griffin, Affiliate Associate Professor of Earth Sciences, UNH/Associate Professor of Civil and Environmental Engineering, Rice University

Kelley C. Barsanti, Visiting Scientist, Atmospheric Chemistry Division, National Center for Atmospheric Research

Jack Dibb, Research Associate Professor, Complex Systems Research Center and Department of Earth Sciences, UNH

August 20, 2009

Date

ACKNOWLEDGEMENTS

Funding for this project was provided by both the Houston Advanced Research Center (HARC) and the UNH Department of Earth Sciences. I would like to extend my thanks to everyone who helped me throughout this project and especially to Luke Ziemba and Pat Wilkinson for their constant guidance and assistance. Special thanks goes to my advisor, Rob Griffin, who provided invaluable support and advice that I could have never done without, and to my committee members, Kelley Barsanti and Jack Dibb, for their helpful insight and comments. Lastly, I would like to thank all of my friends, family, and most of all, my parents, whose constant encouragement always helped me to believe in myself.

TABLE OF CONTENTS

LIST OF TABLES

LIST OF FIGURES

ABSTRACT

ANALYSIS OF ORGANIC AEROSOL IN HOUSTON, TX, THROUGH AEROSOL MASS SPECTROMETRY AND PROTON NUCLEAR MAGNETIC RESONANCE SPECTROSCOPY

By

Meredith J. Cleveland

University of New Hampshire, August 2009

Organic aerosol from Houston, TX, was measured during August and September of 2006 as part of the Texas Air Quality Study II Radical and Aerosol Measurement Project. Aerosol size and composition were determined using an Aerodyne quadrupole aerosol mass spectrometer, and twenty-nine aerosol filter samples were analyzed using proton nuclear magnetic resonance (H-NMR) spectroscopy to determine the relative concentrations of functional groups. Results indicate that changes in Houston aerosol are due to anthropogenic activities resulting in hydrocarbon-like organic aerosol (HOA). Aerosols are less oxygenated than those observed in previous studies, with smaller concentrations of unsaturated groups, and do not fit H-NMR source apportionment fingerprints used for identification of secondary organic aerosol, marine organic aerosol, and biomass burning organic aerosol. It is recommended that a new fingerprint for highly urbanized locations be established utilizing these data and those from other large, polluted cities.

CHAPTER I

INTRODUCTION

Atmospheric aerosols are an important and growing area of research within the scientific community. Aerosols, or particles, are important globally for a variety of reasons, including their part in the global radiation budget and their documented effects on human health. Recent research has focused on quantifying the climate forcings related to particulate matter, as fine (diameter < 2.5 μm) aerosols are known to perturb regional and global climate both directly through scattering and absorption and indirectly through serving as efficient cloud condensation nuclei (IPCC, 2007). These cloud-aerosol effects are characterized as having "medium to low" scientific understanding (IPCC, 2007), underscoring the need to accurately identify their interactions in the atmosphere to improve both regional and global models of climate and air quality. Increased levels of particulate matter have been linked to increased cases of cardiovascular health problems and to increased rates of premature mortality (Pope, 2000).

Aerosols either are emitted directly to the atmosphere (primary aerosols) or formed in secondary chemical reactions (secondary aerosols). While the processes leading to secondary inorganic aerosol production are well understood, those leading to formation of secondary organic aerosol (SOA) are still poorly characterized, due to the large number of volatile organic compounds (VOCs) from a variety of both natural and

anthropogenic emission sources that can participate. Modeling attempts to predict formation of SOA under ambient conditions have yet to quantify accurately SOA mass distributions and physical characteristics (de Gouw et al., 2005).

Many recent studies have focused on organic aerosol (OA), as organic compounds ubiquitously constitute a significant fraction of the total aerosol mass (Zhang et al., 2007; de Gouw et al., 2008). New techniques, such as aerosol mass spectrometry (AMS), have greatly advanced the ability to separate components of OA, namely primary OA (POA) and SOA, on a high resolution time scale (Zhang et al., 2005a,b). Additional efforts to better understand aerosol organic carbon (OC) utilize proton nuclear magnetic resonance (H-NMR) spectroscopy. Based on chosen extraction techniques, H-NMR only analyzes subsets of OC sampled on a filter. For example, H-NMR performed on a water extract characterizes only the water-soluble component of OC, known as WSOC. WSOC has been shown to comprise of 20 – 70% of the aerosol carbon and to impact significantly its hygroscopicity (Saxena and Hildemann, 1996). In many cases, WSOC is also believed to be related to SOA (Hennigan et al, 2008). Specifically, H-NMR illustrates the changes in the oxidation state of aerosol through differences in the functional group budget (Moretti et al., 2008), which can be used as a source apportionment tool to fingerprint different types of OA (Decesari et al., 2007). To date, little research has used tandem measurements from AMS and H-NMR.

In urban centers, where the sources of VOCs and precursors of inorganic secondary aerosol (NO_x and SO_2) are abundant, both primary emission and secondary production of aerosols are important. Houston, TX, where this study occurred, is a heavily populated and industrialized location. Air quality in this region is notably

impacted by high levels of ozone (Kleinman et al., 2002) and particulate matter, especially in the submicron mode (Bates et al., 2008). Common industrial activities in the Houston metropolitan area are related to both petrochemical and power generation facilities, of which a large number are located on the Houston Ship Channel. Flight measurements from summer of 2006 reveal that over 60% of the aerosols in plumes from the Houston Ship Channel are OA (Bahreini et al., 2009, in press). The research performed for this thesis will provide an increased understanding of the nature and dynamics of OA in the Houston atmosphere.

CHAPTER II

METHODS

Field Site Description

Measurements were made in Houston, TX, from August 15 through September 28 of 2006 during the Texas Air Quality Study II (TexAQSII) Radical and Aerosol Measurement Project (TRAMP). All instrumentation was located on top of the North Moody Tower, an 18-story residence hall located on the campus of the University of Houston. The University of Houston is located centrally within the major Houston metropolitan area. It is encircled by the regional highway network and is situated a few kilometers southeast of Houston downtown. It is also situated to the southwest of the highly industrialized Houston Ship Channel. Measurements were performed between mid August and the end of September 2006, a time characterized by high temperatures, high relative humidity, and strong insolation in southeast Texas. All times used in the following studies are in Central Standard Time (CST).

Q-AMS

Particle size and non-refractory mass concentrations were measured with an Aerodyne quadrupole AMS (Q-AMS) and averaged to a temporal resolution of ten minutes. Information regarding instrument design and deployment and the associated data analysis has been described elsewhere (Jayne et al., 2000; Jimenez et al., 2003, Canagaranta et al., 2007), so only a brief description is provided here. Particles with diameters between 0.04 μm and 1.0 μm are focused into a narrow beam by an

aerodynamic lens and are accelerated into a time-of-flight (ToF) chamber. Particle vacuum aerodynamic diameter is determined by the time taken by each particle to traverse this chamber. At the end of the ToF chamber, particles are thermally vaporized at a temperature of ~600°C; vaporized material (non-refractory) is ionized by a 70-eV electron impact ionization source and directed into a quadrupole mass spectrometer where chemical composition is identified quantitatively. The Q-AMS determines signals at unit resolution for mass-to-charge ratios (m/z) between 1 and 300.

Q-AMS data at specific m/z are used to determine mass concentrations of chemical species including nitrate, sulfate, ammonium, chloride, and total organics (Allan et al., 2004). For example, particle-phase nitrate is quantified primarily through addition of the signals at m/z 30 (NO^+) and m/z 46 (NO^+_2), the sum of which account for most of the total nitrate signal. However, it has been suggested recently that the technique for estimating nitrate is complicated by the contribution of organic compounds that also produce signal at m/z 30 (CH_2O^+), leading to an overestimation of particle-phase nitrate (Bae et al., 2007). No correction to account for this interference is made in the data presented here.

The Q-AMS data analysis produces only a total organic mass concentration based on the assumption that any signal not derived from gases (air, water, etc.) or known inorganic species is derived from organic material. Because this method does not allow for the classification of any specific constituents of OA, a component analysis technique for de-convoluting the total organic spectra has been applied to the dataset (Zhang et al., 2005a, b). The OA is separated into two types: hydrocarbon-like OA (HOA) and oxygenated OA (OOA). This method was developed for Pittsburgh urban aerosols but

has been used successfully for Houston aerosols (Zhang et al., 2007). It has been shown that HOA and OOA can be used as proxies for POA and SOA, respectively (Zhang et al., 2005b). HOA and OOA are linked closely to the common spectral tracers m/z 57 and m/z 44, respectively.

Recently, more advanced models have been applied to Q-AMS datasets resulting in additional sub-components for OOA. Frequently, these new components are distinguished by varying amounts of oxidation (Ulbrich et al., 2009). However, the simpler two-component model was deemed applicable for the current study due to evidence of decreased processing in the TRAMP aerosols and the previous success of the two component model in Houston (Zhang et al., 2007).

Proton Nuclear Magnetic Resonance (H-NMR)

Size-segregated aerosol samples (particle diameters < 2.5 μm) were collected with a Versatile Air Pollutant Sampler (VAPS, University Research Glass, URG, Chapel Hill, North Carolina) onto quartz-fiber filters (pre-fired, 47-mm diameter Pallflex® Tissuquartz, Pall Life Sciences, East Hills, New York) as described in Ziemba et al. (2007). Briefly, aerosols enter a virtual impactor to remove particles larger than 10 μm in diameter and are sent into three separate channels, two designated for fine particles and one for coarse (particle diameters between 2.5 and 10 μm). One fine particle channel was used to analyze inorganic chemical constituents, while the other was selected for organic species. Both channels utilized a flow rate of 15 L min^{-1} throughout the campaign. Samples for this analysis were chosen from the organic fine particle channel.

Filters were changed regularly throughout the campaign approximately every 12 hours, with few exceptions. Specific samples were chosen for this investigation based on

the analysis of concurrent Q-AMS data and on including equal numbers of day and night samples to allow for a diurnal analysis. Additional samples chosen include days that exhibited large m/z 44 and 57 signals in the Q-AMS spectra and special time resolution samples taken during pre-morning rush hour and rush hour. Overall, 29 out of the 86 samples collected during TRAMP were chosen for further analysis.

From each filter, two 1.5-cm^2 punches were soaked in 5 mL of ultrapure (milliQ) water for 10 minutes and then centrifuged for an additional 10 minutes. Aliquots of the centrifuged solution were freeze-dried until all liquid was evaporated and then re-dissolved with 0.8 mL of high purity (99.999%) D_2O.

H-NMR analysis was performed using a Varian Inova 500 MHz NMR with an inverse probe. All samples were run for 1024 scans using a PRESAT pulse sequence to suppress the residual HOD peak. A 0.5 Hz line-broadening function was applied, as were six sequential polynomial baseline corrections. The spectra were integrated in specific regions to quantify hydrogen atoms and the resulting functional groups based on the analysis of Tagliavini et al. (2006). The functional groups are as follows: 0.60 – 1.80 ppm (aliphatic hydrogens, R-H); 1.80 – 3.20 ppm (hydrogens in α-position to unsaturated carbons, =C-C-H); 3.20 – 4.40 ppm (hydrogens bound to alcoholic, ethereal, or estereal carbons, O-C-H); 5.00 – 5.50 ppm (acetalic and vinylic hydrogens, O-CH-O and =C-H); and 6.50 – 8.20 ppm (arylic hydrogens, Ar-H).

To better compare to previous studies, the concentrations of organic hydrogen provided by H-NMR spectroscopy were converted to organic carbon concentrations via the hydrogen-to-carbon (H/C) ratios for each functional group provided by Decesari et al. (2007). Additionally, ketone and carboxylic aliphatic groups (H-C-C=O) were estimated

by utilizing the measured H-C-C= and H-Ar (assumed to be proportional to the benzylic content of the sample) signals. Here, it was assumed that the H-C-C=O content was equal to the difference between the H-C-C= signal and that of the benzylic groups. Similar methods can be used to calculate oxygen-to-carbon (O/C) ratios. In this study, the two oxygenated functional groups (unsaturated and hydroxyl) were utilized to estimate the O/C ratios for the water-soluble fraction. A ratio of 1.5 was applied to the unsaturated groups, including both carboxylic acids and ketones, while the hydroxyl groups were estimated to have an O/C of 1.

No standards were used in this analysis. Therefore, it should be noted that no mass concentrations of functional groups are calculated. Typical error calculations are also unavailable. The contribution of a functional group within a sample is normalized to the total signal, and the intensities of the listed functional groups are displayed relative to one another.

Supplementary Measurements

Additional supporting gas-phase and meteorological data were also acquired on the roof of Moody tower (Lefer and Rappenglück, in press). A 10-meter sampling tower at the top of the facility housed all meteorological instrumentation as well as a suite of air chemistry measurements. Measurements at this location are thought to be representative of Houston's urban boundary layer and not impacted directly by surface level emissions due to the height of the sampling location.

Carbon monoxide (CO) data utilized in this study were collected with a TEI 48c trace-level enhanced gas filter correlation wheel instrument. All VOC data were collected with a Perkin-Elmer VOC system, which was online for the duration of the

TRAMP campaign (Leuchner and Rappenglück, 2009, in press). Nitrate radical data were collected using a long-path differential optical absorption spectrometer (LP-DOAS), details of which are reported in Wang et al. (2006).

CHAPTER III

RESULTS AND DISCUSSIONS

AMS Aerosol Composition

Table 1 lists statistics for ammonium, nitrate, sulfate, organics, and chloride for the entire campaign. The aerosol composition in Houston during TRAMP is dominated by sulfate and organic material, with considerably smaller fractions of ammonium and nitrate. All species have a mode in the mass-based size distribution at approximately 300 nm in vacuum aerodynamic diameter (with occasional smaller modes ranging from 100 nm to 150 nm, and for organics, even down to 70 nm). Large mass loadings of organic material and sulfate often occur during the same periods during the campaign, but some occasions indicate sulfate dominating without a corresponding organic signal. Ammonium correlates strongly to sulfate for the entire campaign (Figure 1), and the regression indicates aerosol that is not fully neutralized with respect to ammonium (the 1:2 line).

Sulfate

Sulfate accounts for an average of 38% of the total measured aerosol mass during the TRAMP campaign, with a mean concentration of 4.08 ± 2.62 $\mu g\ m^{-3}$. The average to median ratio is 1.2, indicating that aerosol sulfate at the TRAMP site is a regional phenomenon that is not unduly influenced by a specific source. However, there are certain times when increases in SO_2 and sulfate occur concurrently, possibly showing that

SO_2 plumes moving past the Moody Tower impact sulfate formation. These times are not representative of the majority of the dataset. Hourly medians show a distinct diurnal profile, with a strong peak at 3pm and a smaller peak at 9pm. The minimum occurs at approximately 7am. The afternoon peak is consistent with sulfate forming through photochemical channels: aqueous conversion of S(IV) to S(VI) or reactions of SO_2 with the hydroxyl radical.

Ammonium

Ammonium comprises 8.5% on average of the total measured aerosol mass during TRAMP, with a mean concentration of 0.92 ± 0.52 μg m^{-3}. The median to average ratio is 1.1, similar to sulfate. The regression between the molar concentrations of ammonium and sulfate produce a slope of 0.8 (see Figure 1), closer to that of ammonium bisulfate (slope of 1) than ammonium sulfate (slope of 0.5). Production of ammonium bisulfate is representative of aerosols that are likely acidic; here, the aerosols sampled are more acidic than those measured with a Q-AMS in New Hampshire and Pittsburgh (Cottrell et al., 2008; Zhang et al., 2005b) consistent with a location with significant SO_2 emissions but relatively small emissions of NH_3.

Nitrate

Nitrate concentrations during TRAMP were small, with a mean of 0.38 ± 0.45 μg m^{-3}, accounting for only 6% of the total average measured mass. Ammonium nitrate would not be expected to form due to the acidic nature of the aerosols in Houston and the high temperatures in this location during the summer. More evidence that this nitrate is not ammonium nitrate is demonstrated in the ratio of the signal at m/z 46 to that at m/z 30. For ammonium nitrate, this ratio is approximately 1:2; deviations from this value

signify the contribution of other forms of nitrate. For organic nitrates, this ratio has been shown to decrease considerably, with a ratio of approximately 1:10 for SOA formed from the reaction of the nitrate radical with β-pinene (Fry et al., 2009) and 1:5 and 1:8 for SOA formed from α-pinene and 1-3-5 trimethylbenzene, respectively, undergoing photooxidation in the presence of NO_x (Alfarra et al., 2006). The average ratio during TRAMP is 1:4.5, representative of nitrate in a form other than ammonium nitrate. It is postulated that the nitrate is most likely organic due to the large emissions of VOCs and POA in Houston. It is also possible that the AMS-derived nitrate suffers from interference of signal from CH_2O^+. Additionally, the relationship between the molar nitrate concentration and the ratio of the molar concentrations of ammonium to sulfate indicate that significant, if not most, nitrate mass is forming when the ammonium to sulfate ratio is less than two. This result has been observed in other locations (Cottrell et al., 2008) and suggests that traditional pure solution thermodynamics cannot be used solely to predict nitrate formation.

Organics

Organics constituted the majority of the particulate matter measured by the Q-AMS, with a mean of 5.46 ± 4.00 μg m^{-3}, accounting for slightly more than 50% of the total average mass. The average to median ratio is close to unity as there are a large variety of sources of organic material at the TRAMP site in almost all directions. Total mass of organic material showed a diurnal trend with hourly means and medians approximately equal. A distinct peak in mass is evident at 8AM, concurrent with large POA emissions due to Houston morning rush hour. A smaller, less distinct peak occurs

at 3PM, at the height of photochemical oxidation, although it is not echoed by the hourly 95th percentiles.

The average organic mass spectrum for the entire campaign is presented in Figure 2. Enhanced signals at m/z 27, 29, 41, 43, 55, 57, and 69 are consistent with those from urban environments (Zhang et al., 2005a). The enhanced signal at m/z 44 indicates the presence of OOA.

OOA/HOA Analysis

Time series of HOA and OOA for the entire TRAMP campaign are presented in Figure 3. The average HOA is 1.74 ± 1.90 μg m^{-3}, accounting for 32% of the total OA. The average OOA concentration is 3.74 ± 2.63 μg m^{-3}. Diurnal trends in the data are observed, with HOA strongly peaking at approximately 8AM, coinciding with Houston morning rush hour (Figure 4). There is also another smaller peak in the diurnal HOA trend at approximately 2 am (making up 39% of the total OA at that time, only 5% lower than the rush hour peak). The most probable reason for this peak is nighttime industrial emissions from the many varied sources in the Houston area (Leucher and Rappenglück, in preparation).

OOA has a less pronounced diurnal trend, with small increases at approximately 8 am (once again due to morning rush hour emissions) and again at 3 pm, when photochemical oxidation is at its highest. OOA comprises approximately 80% of the total OA during this afternoon peak. It should also be noted that these increases in OOA occur during the times of greatest dilution, indicating the importance of photochemical aerosol formation at this location.

In Table 2, results of linear regressions of the resulting average HOA and OOA spectra with common POA and SOA spectra are shown. The r^2 values for HOA versus published Pittsburgh HOA values, diesel exhaust aerosols, lubricating oil, and diesel fuel from a laboratory study are all 0.77 or greater. Additionally, time series data for HOA were correlated with the Q-AMS measured species of sulfate, ammonium, and nitrate as well as CO, a common anthropogenic tracer of motor vehicular and combustion emissions. The HOA time series tracks CO ($r^2 = 0.51$) and nitrate ($r^2 = 0.45$), while the HOA spectra exhibits enhanced signals at m/z 43, 55 and 57, which is consistent with POA (Zhang et al., 2005 a,b).

The r^2 values for the OOA spectra versus spectra from Pittsburgh OOA, chamber SOA, rural OA from Vancouver, Canada, and fulvic acid all are 0.81 or greater, representative of aerosol that likely secondary. However, the OOA time series shows a fairly weak correlation with sulfate ($r^2 = 0.23$), possibly indicating that Houston OOA is less processed or "aged" and is less regional in nature. A regression between Pittsburgh OOA and sulfate yields an $r^2 = 0.75$, typical for a location that receives highly processed aerosols due to air mass advection (Zhang et al., 2005b). Similarly, the more oxidized OOA component from rural New Hampshire is strongly correlated to sulfate with an r^2 of 0.74 (Cottrell et al., 2008). Decreased signals at m/z 18, 44, and 55 compared to rural OA are also indicative of less oxidized OOA. It is most likely that Houston OOA, while still secondary, is significantly less processed. This has been suggested previously for Houston aerosols. Analysis of aerosols collected aboard the RV *Ronald H. Brown* in 2006 (collected concurrently with the TRAMP field campaign) suggests that

comparatively less atmospheric aging of aerosols occurs in the region based on the lack of increases in measured O/C ratios (Russell et al., 2009).

Analysis of Nighttime Organic Events

Recent investigation into Houston nocturnal chemistry indicates the potential for nocturnal SOA formation (Stutz et. al, in press, b). While the importance of the OH radical decreases at night, other oxidants such as the nitrate radical ($NO_3^{\bullet}$) become important. Reactions of $NO_3^{\bullet}$ with unsaturated hydrocarbons such as isoprene have been proven to form SOA in chamber experiments (Ng et al., 2008) and to form more SOA nocturnally than reactions with available OH or O_3 (Brown et al., 2009). Interestingly, isoprene is also responsible for up to 70% of the nocturnal $NO_3^{\bullet}$ loss during TRAMP (Stutz et al., in press, b). Therefore, OA nocturnal mass loadings were investigated to identify any discernable changes in Q-AMS measured OA due to the $NO_3^{\bullet}$/isoprene reaction.

OA nocturnal "events" were found to be fairly common in the Houston Q-AMS dataset. These events are characterized by large, sustained increases in OA starting after dark and ending before the start of morning rush hour on the following day. To analyze these events further, specific criteria were applied to select events with the potential for nitrate chemistry. First, all events occurred between 9 pm and 4 am to ensure the event was after sunset and not affected by Houston morning rush hour. Second, sulfate concentrations remained constant or decreased throughout the duration of the events to remove from consideration increases in OA mass related to other processes. Lastly, OA mass increased by a net minimum of 1 $\mu g\ m^{-3}$ over the constant background of OA mass present in Houston.

For this analysis, six events were identified based on the listed criteria. These events occurred on 8/20, 8/29, 9/2, 9/3, 9/14, and 9/19. The specific times and duration of these events are shown in Table 3. Many of these events occur on days dominated by high pressure (indicating stagnancy) and high pollution but also occur before four of the HONO morning rush hour formation events described by Ziemba et al. (2009, in press). Additionally, the events were further classified into categories based on differences found in the mass spectra. These categories include aerosols that appear to be influenced by combustion (9/14 and 9/19) and those influenced by oxidation and possibly biomass burning (8/29, 9/2, and 9/3). The event on 8/20 is discussed separately due to its individual characteristics.

Combustion Events

The 9/14 and 9/19 events are characterized by large increases in OA mass that occur suddenly over a few hours. The calculated HOA and OOA traces show that both events display increases in HOA, while the 9/19 event also indicates increases in both HOA and OOA (Table 3). The 9/19 event has the highest concentration of OA in the entire dataset. Similarly, the average HOA and OOA during these two events were higher than the campaign averages by approximately by 6 $\mu g\ m^{-3}$ and 2 $\mu g\ m^{-3}$, respectively. HOA is generally increasing more rapidly compared to OOA, which also is shown in the ratio of OOA/HOA. The campaign-average value of this ratio was slightly larger than two, while the average for these two events was approximately one.

Furthermore, these spikes in OA mass appear to be well correlated with changes in wind direction. Figure 5 represents a typical event, showing changes in wind direction that correlate with large increases in HOA relative to OOA. While there is no specific

wind direction that appears to consistently correlate positively with increases in OA mass, the sector between 0-90 degrees occurs in four out the six events and in one out the two combustion events (Table 3). The 0-90 degree range corresponds with wind flow moving over the polluted Houston Ship Channel. Therefore, it can be surmised that the dramatic changes observed in HOA throughout the events are most likely being produced in this region. It can also be observed in Figure 5 that the potential source may be temporally variant as shifts to the same wind direction later in the event do not produce corresponding large increases in OA mass concentrations.

When examining the mass spectra during these two events, certain identifiable m/z signals are enhanced significantly (Figure 6). For example, m/z 57 is enhanced in both events, along with m/z ratios at intervals of 12 and 14 corresponding with m/z 69, 71, 81, 83, 85, 93, 95, and 97, associated with the addition of C^+, CH_2^+... These fragments are also prominent in Houston morning rush hour aerosol (Ziemba et al., 2009, in press). This fragmentation pattern is typical for primary aerosols produced in combustion activities (Zhang et al., 2005b).

When the 9/14 and 9/19 events were examined for evidence of nitrate chemistry, the results were inconclusive. Mass concentrations of nitrate increased in both events, and both events show decreases in the ratio of m/z 46 to m/z 30 compared to the nighttime average ratio of 0.23, possibly indicative of organic nitrate formation. However, the ratios of O/C calculated for the events (using the technique of Aiken et al., 2008) show little deviation from the nighttime average (0.32). For these two events, the O/C ratios were 0.37 and 0.28. This is consistent with results from a similar analysis for aerosols sampled on the RV *Ronald H. Brown* at the same time near Houston (Russell et

al., 2009). If organic nitrogen is contributing to the nitrate signal via formation of SOA, it is not producing a corresponding increase in the O/C ratio calculated based on the technique of Aiken et al. (2008). For comparison, more oxidized aerosols, like those associated with SOA, exhibit O/C ratios in the range of 0.52 to 0.64, and those associated with biomass burning (BB) have ratios of approximately 0.30. HOA typically has the smallest O/C, with a range of 0.06 to 0.10 (Aiken et al., 2008). The results from the two nocturnal combustion events are similar to those that are characteristic of BB, although there is no evidence of BB in the mass spectra. Neither ratio suggests significant oxidation that would be associated with SOA produced in the $NO_3^{\bullet}$/isoprene reaction.

Biomass Burning/Oxidation Events

These events are also characterized by large increases in OA mass over a few hours and are well correlated with wind direction. All three "oxidation" events on 8/29, 9/2, and 9/3 correspond with wind flow coming from the 0-90 degree sector. However, unlike the combustion events, the HOA mass is increasing but the total OA mass is still primarily composed of OOA. The average OOA/HOA ratio during the oxidation events is 2.39, slightly larger than the campaign average and significantly larger than those of the combustion events. Moreover, there is evidence in the mass spectra of sources other than industry. While some of the m/z ratios of 57, 69, 71, 81, 83, 85, 93, 95, and 97 are enhanced during the oxidation events, enhancement also occurs at m/z 60 and 73 and the associated fragments at 87, 100, and 114 (Figure 7). The signals at m/z 60 ($C_2H_4O_2^+$) and 73 have been associated with levoglucosan and carboxylic acids, markers for BB (Aiken et al., 2008). These fragments are depleted in Houston morning rush hour aerosols (Ziemba et al., 2009, in press) and not observed in other diesel and urban aerosols (Zhang

et al., 2005a), pointing to the possibility that the events on 8/29, 9/2, and 9/3 are not completely comprised of typical urban primary aerosol.

However, O/C ratios calculated for the oxidation events are all approximately equal to the nighttime average, again appearing similar to BBOA rather than SOA. The m/z ratio of 46/30 decreases in two out of the three oxidation events, but the decreases are not significant enough to postulate that organic nitrates are contributing to SOA.

8/20 Event

The event on 8/20 is not similar to the combustion nor the oxidation events. HOA increases during this event more significantly than all the other events, with an OOA/HOA ratio of 0.20, far smaller than the campaign average and the averages of both event categories. This indicates that the event is dominated by primary emissions, which is confirmed by the smallest O/C value of all the events (0.16), falling close to the "HOA-like" classification of Aiken et al. (2008).

Perhaps most intriguing, however, is the lack of evidence in the average mass spectrum for any deviations from an average non-event night. Most m/z ratios are not enhanced, not even m/z 57, which is strongly associated with primary combustion aerosol. Enhancements occur in the large organics (Figure 8), between m/z 200 and 300, specifically for nine out 14 m/z ratios associated with eight polycyclic aromatic hydrocarbons (PAH) identified in Mexico City (Dzepina et al., 2007). PAHs are formed through a wide variety of combustion activities and come from a variety of sources, including diesel fuel, gasoline combustion, and BB. However, these PAHs (grouped as m/z 202, 216, 226+228, 240+242, 250+252, 264+266, 276+278, and 288+290) are enhanced in every event, not only on 8/20. The same PAHs are not enhanced every

time, but at least six out of the 14 associated fragments are always enriched. There is no apparent pattern of enhancement or grouping of PAH signals between events or categories, though the signals at 264+266 and 288+290 are less frequently enhanced than the others. These specific groupings were also not enriched in Houston morning rush hour aerosol (Ziemba et al., 2009, in press). Additionally, the m/z 46/30 ratio indicated no evidence of organic nitrate in the mass spectra.

Analysis of Nitrate Chemistry

Throughout the TRAMP campaign, nighttime chemistry between the nitrate radical and VOCs was very active (Stutz et al., in press, b). While mass concentrations of nitrate increased in five out of the six nocturnal events, only three out of five events had decreases in the ratio m/z 46 to m/z 30 from the nighttime average of 0.23. Additionally, linear regressions performed between OA during events and common VOCs show significant correlation with r^2 coefficients greater than 0.6 for acetylene, benzene, and toluene (Table 4). Acetylene is commonly used as a tracer for anthropogenic activities, and both toluene and benzene are also the result of industrial activities associated with the petroleum industry. Isoprene and 1-3-butadiene (responsible for the bulk of the remaining $NO_3^{\bullet}$ loss) generate r^2 coefficients of 0.06 and 0.33, respectively. However, the reactions forming SOA from the products of the $NO_3^{\bullet}$/isoprene reaction are non-linear and therefore may not display high r^2 coefficients.

In general, isoprene/nitrate chemistry does not appear to play a significant role in increasing OA concentrations at night in Houston. SOA yields determined for the isoprene/ $NO_3^{\bullet}$ reaction from chamber experiments indicate that the mass created in this reaction would be small, even with large amounts of isoprene present (Ng et al., 2008).

When applying this yield to the conditions present during events, amounts of SOA formed (ranging from 0.1 μg to 1 μg) are most likely too small to distinguish using the Q-AMS in comparison to the large background of OA mass present in Houston.

H-NMR Analysis

The average of all spectra measured using H-NMR on the water extract from the 29 filter samples is presented in Figure 9. Identification of specific peaks in this spectrum is difficult because of the large number of compounds that constitute aerosol particles. In Figure 9, the large disturbance at approximately 5 ppm is the residual HOD peak, while the other largest peaks present occur in the aliphatic portion of the spectrum. A maximum at 0.9 ppm is in the range of methyl groups (0.7 – 1.0 ppm) and another peak at 1.2 falls in the range of chain methylene groups (1.2-1.8 ppm) (Decesari et al., 2000). These correspond to alkyl carbon with low reactivity with respect to most atmospheric oxidants except OH (Moretti et. al, 2008). Smaller intensities are seen between 1.8 and 4.40 ppm, which includes hydrogen attached to carbon in the α-position to unsaturated carbons (1.8 – 3.20 ppm) and hydrogen bound to carbon associated with alcohols, esters, and ethers (3.20-4.40 ppm). Trace amounts of anomeric (5 – 5.50 ppm) and aromatic (6.50 – 8. 2 ppm) carbon exist only in a few samples. Anomeric carbon was observed in only three (out of 29) samples, while aromatic carbon was observed in seven samples. The peak of aromatic hydrogen in Figure 9 results from one very large outlier influencing the average. Trace levels of aromatics were associated with the three samples in which anomeric carbon was measured. While the lack of anomeric carbon is common in previous studies, contributions from aromatics have been identified frequently in aerosol samples (Decesari et al., 2000; Tagliavini et al. 2006; Decesari et al., 2007;

Moretti et al., 2008). In this case, it is possible that aromatics in POA reacted quickly due to the high oxidative capacity in the Houston atmosphere and that the products of these reactions did not retain their aromatic structure. Given the relatively slow heterogeneous oxidation rates (lifetimes approaching several days) thought to occur in the atmosphere (Weitkamp et al., 2008), this seems unlikely. It is also possible that SOA formed from aromatic VOCs is formed from products that do not retain their aromatic nature. Finally, it should be noted that these analyses were performed on water-soluble material. The low solubility of non-functionalized aromatic species in POA also could contribute to the lack of an aromatic signal. Of the seven samples in which aromatics were measured, six were collected during the day.

To investigate the differences between the samples with and without aromatic/anomeric carbon reported, the samples with aromatics are presented compared to the campaign average in Figure 10. A small decrease in aliphatic carbon is observed, as is a large decrease in the unsaturated functions. A corresponding increase is shown in the hydroxylic functions. These characteristics correlate with aerosol that is fresh and unprocessed (Moretti et al., 2008). Also of note is that all of the aromatic samples correspond with fairly polluted days in Houston as defined by Stutz et al. (in press, a).

Aerosols analyzed using H-NMR from a site 40 km outside of London were characterized by large contributions from alkyl carbon and hydroxyl groups, while biogenic SOA displayed decreased levels of hydroxyl groups (Decesari et al., 2007). In general, Houston samples appear similar to anthropogenic aerosols, with large contributions from alkyl and alcohol groups. The level of alkyl content remains steady in most of the measured samples, comprising approximately 63% of the aliphatic carbon

signal (sum of alkyl, unsaturated, and hydroxyl groups). In comparison, the contribution of ketone and carboxylic groups fluctuated significantly from sample to sample, by up to an order of magnitude. In total, they represented between 0 to 40% of the measured signal. Lastly, the hydroxy and alkoxy content varied between 8 and 45% of the measured signal. This is partially consistent with the findings of Decesari et al. (2007) who reported large variability in the hydroxy/alkoxy content but limited changes in the level of carbonyl/carboxyl groups despite sampling air masses from a range of different source regions .

While there are large differences from sample to sample, the variability decreases when comparing average day and night intensities (Figure 11). It must be noted here that while nearly equal numbers of daytime and night samples are included in these calculations, the samples were not always chosen from the same specific day. The variability from sample to sample has been demonstrated to be large and therefore may obscure any true diurnal trend.

Only small differences can be noted in the carbon bound to unsaturated functions and hydroxylic carbon. Anomeric and aromatic carbon are not included due to their negligible contributions. To help emphasize these differences, the day and night averages are presented as ratios to the campaign average in Figure 12. Aliphatic carbon shows no enhancement or depletion based on the time of day. For the carbon bound to unsaturated functions, there is a pronounced nighttime enhancement and resulting daytime depletion. This is opposite what is observed for the hydroxylic carbon, which exhibits daytime enhancements and nighttime depletions. Based on Moretti et al. (2008), it appears that daytime water-soluble aerosols in Houston are influenced to a slightly larger extent by

fresh particles, while those at night appear to be more processed. This is in contrast to what would be expected if photochemistry were driving formation of SOA during the day. It is possible that the daytime samples chosen are smeared by large contributions by POA from rush hour and that the nighttime samples chosen represent residual SOA concentrations on nights when POA concentrations were small.

Similarly, corresponding O/C ratios calculated using the entire Q-AMS dataset do not reveal large changes between day and night. The average daytime ratio is 0.42, while the nighttime average ratio is 0.37, indicating only slightly less oxidation. These ratios are consistent with those calculated on the RV *Ronald H. Brown* in the Houston area during the same time period (Russell et al., 2009) using Q-AMS measurements and Fourier-transform infrared spectroscropy. It was suggested that aging of aerosols in Houston occurs rapidly and is not photochemically limited. The results from this analysis corroborate this theory.

The O/C ratios calculated using the Q-AMS data were compared to those calculated using the H-NMR functional groups even though slight differences in particle size sampled could cause small differences in the results. In addition, it must again be stressed that the H-NMR results represent only the water-soluble fraction of OA. Generally, the Q-AMS O/C ratios were larger than the H-NMR O/C values, with an average Q-AMS/H-NMR ratio of 1.7. The H-NMR O/C values vary from 0.08 to 0.46, while the AMS O/C values range between 0.22 and 0.49. Additionally, the H-NMR O/C values display few differences between day and night, with a daytime average of 0.27 and a nighttime average of 0.29, corroborating the lack of change seen in the Q-AMS O/C day/night averages, even if the values are smaller. While the calculated ratios from both

methods do not directly correlate, the difference between the two ratios decreases with larger values of the H-NMR O/C (Figure 13). This indicates a water-insoluble (based on the extraction method used) OA component with significant O/C being measured by the Q-AMS; this phenomenon should be investigated in the future as increased O/C should indicate increased water solubility.

In an attempt to discern differences in aerosols that are processed versus freshly emitted, single NMR samples were compared for times associated with aerosols that were known to be highly oxidized and vice versa based on the Q-AMS dataset. The filter samples corresponding to the times with the highest m/z 44 and 57 signals were analyzed, as well as the higher time resolution samples corresponding to the time before Houston rush hour ("pre rush-hour", between 21-4 CST) and morning rush hour (4-8 CST). The samples with large m/z 44 and 57 signals show large influences from OOA and HOA, respectively. Due to instrumental issues, there are no corresponding Q-AMS data for the pre-rush hour/rush hour samples. However, morning rush hour is strongly associated with HOA (Ziemba et al., 2009, in press). The results from this analysis are presented in Figure 14. Anomeric and aromatic carbon are once again not included due to negligible contributions. The signals are not presented as ratios to the campaign average due to the larger differences between the samples.

The samples exhibit little change in aliphatic carbon, but large changes occur for both unsaturated carbon and hydroxylic carbon. The m/z 44 sample displays increases in the unsaturated groups and decreases in the hydroxyl group relative to the m/z 57 sample. The opposite is true for the pre-rush hour/rush-hour samples, with the pre-rush hour sample displaying decreases in the ketone/carboxylic acid groups and increases in the

alcohols, esters, and ethers (again, relative to the rush-hour sample). While the trends in the m/z 44 and 57 samples are consistent with what is expected of OOA samples versus HOA samples, the pre-rush hour/rush hour samples display the opposite trend. It is possible that the pre-rush hour sample also is dominated by emissions of HOA, but this cannot be confirmed without corroborating Q-AMS data.

Recently, an effort was made to source apportion aerosols utilizing the fingerprint of H-NMR (Decesari et. al, 2007). In this method, carbonylic/carboxylic groups were estimated by subtracting 1/5 of the aromatics from the unsaturated groups and presented as a ratio to the sum aliphatics, termed as the total signal of the aliphatic, unsaturated, and hydroxyl groups. This ratio was compared to the ratio of hydroxyl groups to the sum of aliphatics using data from multiple sites and influences to create source boundaries for three different types of aerosol: marine OA, SOA, and BBOA. This method was applied to the H-NMR samples from TRAMP, and results are plotted with the three corresponding source boxes in Figure 15. The points in this figure are colored using the NMR O/C ratios.

The TRAMP samples in Figure 15 clearly vary significantly from the three established source regions, especially in the contribution of carbonylic/carboxylic groups, underscoring the lack of oxidation present in the aerosols at the TRAMP site. The fractional contribution of hydroxyl groups did not vary outside of the previously determined source regions. Moreover, the NMR O/C ratios accentuate decreasing oxidation with lower concentrations of both unsaturated and hydroxyl groups. The same points colored using the O/C ratios calculated from the Q-AMS dataset do not display similar trends, again highlighting differences between the two techniques.

It should be noted that the fingerprint boxes in Figure 15 result from a composite of over ten locations, but only a few sites had more than two samples. The only polluted location included that had several associated samples (the Po Valley in Italy) showed more variability in both the carbonylic/carboxylic and hydroxylic fractions than all other locations studied. Additionally, while the Po Valley is influenced by pollution sources, it does not have the same type of extreme pollution as an urban/industrial center like Houston. Therefore, the TRAMP variability, while intriguing, is not completely unexpected.

CHAPTER IV

CONCLUSIONS

Aerosol measurements made with a Q-AMS in Houston, TX, during the TRAMP campaign indicate aerosols in this location are primarily comprised of organic material and sulfate, with smaller fractions of ammonium and nitrate. Aerosols in Houston are slightly acidic, with sulfate concentrations that track ammonium closely and nitrate concentrations that follow OA. More specific analysis of the organic portion of the aerosol with multiple component analysis yields an average OA composition is approximately 2/3 OOA and 1/3 HOA. HOA correlates well with common POA tracers, while OOA appears to be well correlated with SOA species. The OOA appears to be formed locally based on a lack of correlation with sulfate.

Investigation of nighttime OA events leads to the conclusion that nighttime OA increases in mass are strongly affected by wind flow over an extremely polluted industrial area. The resulting aerosols show large increases in HOA mass relative to OOA, significantly deviating from the campaign average ratio for OOA/HOA. The aerosol mass spectrum is altered during these events, showing that specific events are influenced strongly by products of combustion processes, while others show effects of biomass burning and oxidation. The O/C ratios generally follow the same trends. The 8/20 event is conspicuously incongruous, displaying an extremely small O/C ratio but

possessing little corresponding evidence in the mass spectrum for enhanced combustion. Certain PAHs appear to be enriched relative to the average night.

While important for the budget of the nitrate radical and VOCs, the nocturnal reactions between the nitrate radical and isoprene do not appear to generate significant OA, at least relative to other OA sources. The ratios of m/z 46/30 show limited evidence of enhanced organic nitrate production, and significant relationships with common industrial tracers support the conclusion that Houston nighttime aerosol events are strongly influenced by anthropogenic activities.

Additionally, H-NMR was performed on 29 samples from the TRAMP campaign. Large variability in comparison to previous studies was noted in both the unsaturated and hydroxyl groups, which tended to co-vary inversely in magnitude in most of the samples. The aliphatic content of the samples remained consistent. Only trace amounts of both anomeric and aromatic carbon were measured, possibly due to the low water solubility of these groups in Houston aerosol.

Averages of day and night samples were compared to ascertain the effects of oxidation on Houston aerosol. While it is expected that daytime photochemical activity should result in higher fractions of unsaturated compared to hydroxyl groups, the reverse trend was observed. The nighttime average presented the opposite result, with higher amounts of unsaturated groups relative to hydroxyl groups. However, calculated O/C ratios for the samples show small changes between day and night and provide little evidence for a diurnal cycle. Therefore, any true diurnal trends may be obscured in Houston by the constant presence of industrial emissions and by the specific samples chosen.

The effects of oxidation were further investigated by utilizing Q-AMS data to choose one sample representative of highly oxidized aerosol (highest concentration of m/z 44 in the TRAMP dataset) and one sample representative of freshly emitted aerosol (highest concentration of m/z 57). These two samples provide validation of the expected trends with high levels of unsaturated groups in the sample dominated by m/z 44 and high levels of hydroxyl groups in the sample with the highest m/z 57. However, two additional higher resolution samples corresponding with pre-rush hour (21- 4 CST) and rush hour (4-8 CST) display the opposite trends of the m/z 44 and m/z 57 samples. Larger signals from hydroxyl groups are present in the pre-rush hour sample, and larger signals from unsaturated groups are observed in the rush hour sample. Due to the lack of Q-AMS data during these higher resolution samples, it cannot be confirmed whether the pre-rush hour period was dominated by HOA, as in several of the nocturnal OA events.

Lastly, the samples were compared to the H-NMR fingerprint established for marine OA, SOA, and BBOA using the source apportionment technique from Decesari et al. (2007). The TRAMP samples displayed a significantly smaller fraction of aliphatic carbon composed of carbonylic/carboxylic groups due to the lower level of oxidation present in Houston aerosol. However, the fraction of aliphatic carbon composed of hydroxyl groups exhibited as much variability as all of the sites in the study of Decesari et al. (2007). As Houston is currently the most polluted city to be examined using H-NMR, the increased variability and lack of oxidation present in the samples is not completely unexpected. This analysis shows that source apportionment utilizing H-NMR only on a water soluble extract may not be applicable in polluted locations due to the large range of functionality in aerosols influenced strongly by POA.

CHAPTER V

RECOMMENDATIONS FOR FUTURE RESEARCH

In order to better understand the processes that form aerosol, it is necessary to fully determine particle composition. Recent advances have been made through the use of aerosol mass spectrometry, allowing for the measurement of inorganic and organic aerosol species with high time resolution. However, the details of the organic fraction of the aerosol remain poorly characterized. Therefore, techniques like nuclear magnetic resonance spectroscopy, used to identify the functional groups comprising an aerosol sample, could prove very beneficial when employed in tandem with an AMS.

Specialized instrumentation is perfect for a site such as Houston, where thousands of anthropogenic sources combine to create aerosols clearly different from many other locations in which measurements have been performed. Better speciation of organic aerosol is needed in this type of polluted location, where emission of primary organic aerosol is significant, oxidation of primary organic aerosol is rapid (though apparently slight), and formation of secondary organic aerosol occurs. The demonstrated variability at the Houston site exhibits the necessity for further measurement in determining the effects and amount of secondary processing of aerosols at this location. Future work should include additional H-NMR analyses on samples collected concurrently with AMS data to better parse the differences between oxidized and non-oxidized aerosol, as well as H-NMR analyses on samples collected at specific times, such as rush hour and the peak

of photochemical activity during the day. Additionally, H-NMR analyses should be performed on samples collected in other polluted cities to determine whether the variability observed in this study is present in other locations. It is also recommended to perform H-NMR on extracts generated using other solvents in addition to water.

LIST OF REFERENCES

Aiken, A. C., P.F. DeCarlo, J.H. Kroll, D.R. Worsnop., J.A. Huffman, K.S. Docherty, I.M. Ulbrich, C. Mohr, J.R. Kimmel, D. Sueper, Y. Sun, Q. Zhang, A. Trimborn, M. Northway, P.J. Ziemann, M.R. Canagaratna, T.B. Onasch, M.R. Alfarra, A.S.H. Prevot, J. Dommen, J. Duplissy, A. Metzger, U. Baltensperger, and J.L. Jimenez (2008), O/C and OM/OC ratios of primary, secondary, and ambient organic aerosols with high resolution time-of-flight aerosol mass spectrometry, *Environ. Sci. Technol., 42*, 4478– 4485, doi:10.1021/es703009q.

Alfarra, M.R., D. Paulsen, M. Gysel, A.A. Garforth, J. Dommen, A.S.H. Prevot, D.R. Worsnop, U. Baltensperger, and H. Coe (2006), A mass spectrometric study of secondary organic aerosols formed from the photooxidation of anthropogenic and biogenic precursors in a reaction chamber, *Atmos. Chem. Phys., 6,* 5279 - 5293.

Allan, J.D., H. Coe, K.N. Bower, M.R. Alfarra, A.E. Delia, J.L. Jimenez, A.M. Middlebrook, F. Drewnick, T.B. Onasch, M.R. Canagaratna, J.T. Jayne, and D.R. Worsnop (2004), Technical Note: Extraction of Chemically Resolved Mass Spectra from Aerodyne Aerosol Mass Spectrometer Data, Journal of Aerosol Science, 35, 909–922.

Bae, M.S., J.J. Schwab, Q. Zhang, O Hogrefe, K.L. Demerjian, S. Weimer, K. Rhoads, D. Orsini, P. Venkatachari, and P.K. Hopke (2007), Interference of organic signals in highly time resolved nitrate measurements by low mass resolution aerosol mass spectrometry, *J. Geophys. Res., 112*, D22, doi:10.1029/2007JD008614.

Bahreini, R., B. Ervens, A.M. Middlebrook, C. Warneke, J.A. de Gouw, P.F. DeCarlo, J.L. Jimenez, C.A. Brock, J.A. Neuman, T.B. Ryerson, H. Stark, E. Atlas, J. Brioude, A. Fried, J.S. Holloway, J. Peischl, D. Richter, J. Walega, P. Weibring, A.G. Wollny, and F.C. Fehsenfeld (in press), Organic aerosol formation in urban and industrial plumes near Houston and Dallas, Texas, *J. Geophys. Res.*, doi:10.1029/2008JD011493

Bates, T.S., P.K. Quinn, D. Coffman, K. Schulz, D.S. Covert, J.E. Johnson, E.J. Williams, B.M. Lerner, W.M. Angevine, S.C. Tucker, W.A. Brewer, and A. Stohl (2008), Boundary layer aerosol chemistry during TexAQS/GoMACCS 2006: Insights into aerosol sources and transformation processes, *J. Geophys. Res., 113,* D00F01, doi:10.1029/2008JD010023.

Brown, S.S., J.A. de Gouw, C. Warneke, T.B. Ryerson, W.P. Dube, E. Atlas, R.J. Weber, R.E. Peltier, J.A. Neuman, J.M. Roberts, A. Swanson, F. Flocke, S.A. McKeen, J. Brioude, R. Sommariva, M. Trainer, F.C. Fehsenfeld, and A.R. Ravishankara (2009), Nocturnal isoprene oxidation over the Northeast United States in summer and its impact on reactive nitrogen partitioning and secondary organic aerosol, *Atmos. Chem. Phys., 9,* 3027-3042.

Canagaratna, M.R., et al. (2007), Chemical and microphysical characterization of ambient aerosols with the Aerodyne aerosol mass spectrometer, *Mass Spectrometry Reviews, 26* (2), 185-222.

Cottrell, L.D., R.J. Griffin, J.L. Jimenez, Q. Zhang, I.M. Ulbrich, L.D. Ziemba, P.J. Beckman, B.C. Sive, and R.W. Talbot (2008), Submicron particles at Thompson Farm during ICARTT measured using aerosol mass spectrometry, *J. Geophys. Res., 113,* D08212, doi:10.1029/2007/JD009192.

de Gouw, J. A., A. M. Middlebrook, C. Warneke, P. D. Goldan, W. C. Kuster, J. M. Roberts, F. C. Fehsenfeld, D. R. Worsnop, M. R. Canagaratna, A. A. P. Pszenny, W. C. Keene, M. Marchewka, S. B. Bertman, and T. S. Bates (2005), Budget of organic carbon in a polluted atmosphere: Results from the New England Air Quality Study in 2002, *J. Geophys. Res., 110,* D16, D16305, doi: 10.1029/2004JD005623.

de Gouw, J. A., C. A. Brock, E. L. Atlas, T. S. Bates, F. C. Fehsenfeld, P. D. Goldan, J. S. Holloway, W. C. Kuster, B. M. Lerner, B. M. Matthew, A. M. Middlebrook, T. B. Onasch, R. E. Peltier, P. K. Quinn, C. J. Senff, A. Stohl, A. P. Sullivan, M. Trainer, C. Warneke, R. J. Weber, and E. J. Williams (2008), Sources of Particulate Matter in the Northeastern United States in Summer: 1. Direct Emissions and Secondary Formation of Organic Matter in Urban Plumes *J. Geophys. Res., 113,* D08301, doi: 10.1029/2007JD009243.

Decesari, S., M.C. Facchini, S. Fuzzi, and E. Tagliavini (2000), Characterization of water soluble organic compounds in atmospheric aerosol: A new approach, *J. Geophys. Res., 105,* D1, 1481–1489.

Decesari, S., M. Mircea, F. Cavalli, S. Fuzzi, F. Moretti, E. Tagliavini, and M.C. Facchini (2007), Source Attribution of Water-Soluble Organic Aerosol by Nuclear Magnetic Resonance Spectroscopy, *Environ. Sci. Technol., 41,* 2479– 2484.

Dzepina, K., J. Arey, L.C. Marr, D.R. Worsnop, D. Salcedo, Q. Zhang, T.B. Onasch, L.T. Molina., M.J. Molina, and J.L. Jimenez (2007), Detection of particle-phase polycyclic aromatic hydrocarbons in Mexico City using an aerosol mass spectrometer. *International Journal of Mass Spectrometry, 263,* 152-170.

Fry, J.L., A. Kiendler-Scharr, A.W. Rollins, P.J. Wooldridge, S.S. Brown, H. Fuchs, W. Dube, A. Mensah, M. dal Maso, R. Tillmann, H.P. Dorn, T. Brauers, and R.C. Cohen (2009), Organic nitrate and secondary organic aerosol yield from NO3 oxidation of beta-pinene evaluated using a gas-phase kinetics/aerosol partitioning model, *Atmos. Chem. Phys., 9,* 1431-1449.

Hennigan, C. J., M. H. Bergin, J. E. Dibb, and R. J. Weber (2008), Enhanced secondary organic aerosol formation due to water uptake by fine particles, *Geophys. Res. Lett., 35,* L18801, doi:10.1029/2008GL035046.

IPCC, 2007: Summary for Policymakers. In: Climate Change 2007: The Physical Science Basis. Contribution of Working Group I to the Fourth Assessment Report of the Intergovernmental Panel on Climate Change [Solomon, S., D. Qin, M. Manning, Z. Chen,M. Marquis, K.B. Avery, M.Tignor and H.L. Miller (eds.)]. Cambridge University Press, Cambridge, United Kingdom and New York, NY, USA.

Jayne, J.T., D.C. Leard, X. Zhang, P. Davidovits, K.A. Smith, C.E. Kolb and D.R. Worsnop (2000), Development of an Aerosol Mass Spectometer for Size and Composition Analysis of Submicron Particles, *Aerosol Science and Technology, 33,* 49-70.

Jimenez, J.L., J.T. Jayne, Q. Shi, C.E. Kolb, D.R. Worsnop, I. Yourshaw, J.H. Seinfeld, R.C. Flagan, X.F. Zhang, K.A. Smith, J.W. Morris, and P. Davidovits (2003), Ambient aerosol sampling using the aerodyne aerosol mass spectrometer, *J. Geophys. Res., 108,* D7, doi:10.1029/2001JD001213

Kleinmann, L.I., P.H. Daum, D. Imre, Y.N. Lee, L.J. Nunnermacker, S.R. Springston, J. Weinstein-Lloyd, and J. Rudolph (2002), Ozone production rate and hydrocarbon reactivity in 5 urban areas: A cause of high ozone concentration in Houston, *Geophys. Res. Lett., 29 (10),* 1467, doi:10.1029/2001GL014569

Lefer, B. and Rappenglück, B. (in press), The TexAQS-II radical and aerosol measurement project (TRAMP), *Atmos. Env.*

Leuchner, M. and Rappenglück, B. (in press), VOC source-receptor relationships in Houston during TexAQS-II, *Atmos. Envi.*

Moretti, F., E. Tagliavini, S. Decesari, M.C. Facchini, M. Rinaldi, and S. Fuzzi (2008), NMR Determination of Total Carbonyls and Carboxyls: A Tool for Tracing the Evolution of Atmospheric Oxidized Organic Aerosols, *Environ. Sci. Technol., 42,* 4844-4849.

Ng, N.L. A.J. Kwan, J.D. Surratt, A.W.H. Chan, P.S. Chhabra, A. Sorooshian, H.O.T. Pye, J.D. Crounse, P.O. Wennberg, R.C. Flagan, and J.H. Seinfeld (2008), Secondary organic aerosol (SOA) formation from reaction of isoprene with nitrate radicals (NO3), *Atmos. Chem. Phys., 8,* 4117-4140.

Pope, C.A (2000),What do epidemiologic findings tell us about health effects of environmental aerosols? *J. of Aerosol Medicine, 13,* 335-354.

Russell, L.M., S. Takahama, S. Liu, L.N. Hawkins, D.S. Covert, P.K. Quinn, and T.S.

Bates (2009), Oxygenated fraction and mass of organic aerosol from direct emission and atmospheric processing measured on the R/V *Ronald Brown* during TEXAQS/GoMACCS 2006, *J. Geophys. Res, 114*, D00F05, doi:10.1029/2008JD011275.

Saxena, P., and L.M. Hildemann (1996), Water-soluble organics in atmospheric particles: A critical review of the literature and application of thermodynamics to identify candidate compounds, *Atmos. Chem. Phys, 1,* 57-109.

Stutz, J. H. Oh, S.I. Whitlow, C. Anderson, J.E. Dibb, J.H. Flynn, B. Rappenglück, andB. Lefer (in press, a), Simultaneous DOAS and mist-chamber IC measurement of HONO in Houston, TX, *Atmos. Envi.*

Stutz, J., K.W. Wong, L. Lawrence, L. Ziemba, J.H. Flynn, B. Rappenglück and B. Lefer (in press, b), Nocturnal NO3 radical chemistry in Houston, TX, *Atmos. Envi.*

Tagliavini, E., F. Moretti, S. Decesari, M. C. Facchini, S. Fuzzi, and W. Maenhaut (2006), Functional group analysis by H NMR/chemical derivatization for the characterization of organic aerosol from the SMOCC field campaign, *Atmos.Chem. Phys., 6*, 1003-1019.

Ulbrich, I.M., M.R. Canagaratna, Q. Zhang, D.R. Worsop, and J.L. Jimenez (2009), Interpretation of organic components from Positive Matrix Factorization of aerosol mass spectrometric data, *Atmos. Chem. Phys., 9,* 2891-2918.

Wang, S., R. Ackermann, and J. Stutz (2006), Vertical profiles of O_3 and NOx chemistry in the polluted nocturnal boundary layer in Phoenix, AZ: Field observations by long path DOAS, *Atmos. Chem. Phys., 6,* 2671-2693.

Weitkamp, E.A., A.T. Lambe, N.M. Donahue, and A.L. Robinson (2008), Laboratory measurements of the heterogeneous oxidation of condensed-phase organic molecular markers for motor vehicle exhaust, *Environ. Sci. Technol., 42,* 7950 7956.

Zhang, Q., M.R. Alfarra, D.R. Worsnop, J.D. Allan, H. Coe, M.R. Canagaratna, and J.L. Jimenez (2005a), Deconvolution and quantification of hydrocarbon-like and oxygenated organic aerosols based on aerosol mass spectrometry, *Environ. Sci. Technol., 39* (13), 4938-4952.

Zhang, Q., D. R. Worsnop, M. R. Canagaratna, and J. L. Jimenez (2005b), Hydrocarbon like and oxygenated organic aerosols in Pittsburgh: insights into sources and processes of organic aerosols, *Atmos. Chem. Phys., 5*, 3289-3311.

Zhang, Q., J. L. Jimenez, M. R. Canagaratna, J. D. Allan, H. Coe, et al. (2007), Ubiquity and dominance of oxygenated species in organic aerosols in anthropogenically influenced Northern Hemisphere midlatitudes, *Geophys. Res. Lett., 34*(13), L13801, doi: 10.1029/2007GL029979.

Ziemba, L.D., E. Fischer, R.J. Griffin, and R.W. Talbot (2007), Aerosol acidity in rural New England: Temporal trends and source region analysis, *J. Geophys. Res., 112,* D10S22, doi:10.1029/2006JD007605.

Ziemba, L.D., J.E. Dibb, R.J. Griffin, C.H. Anderson, S.I. Whitlow, B.L. Lefer, B. Rappenglück and J. Flynn (in press), Heterogeneous conversion of nitric acid to nitrous acid on the surface of primary organic aerosol in an urban atmosphere, *Atmos. Envi.*

Figures

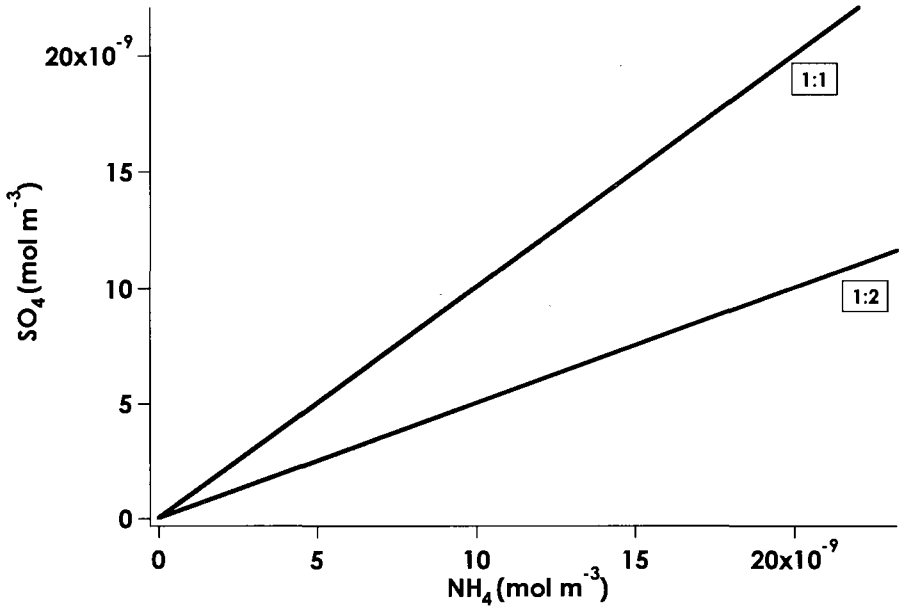

Figure 1 Relationship between molar concentrations of ammonium and sulfate during TRAMP. Points along the x-axis with excess ammonium are representative of one day with low aerosol mass concentrations.

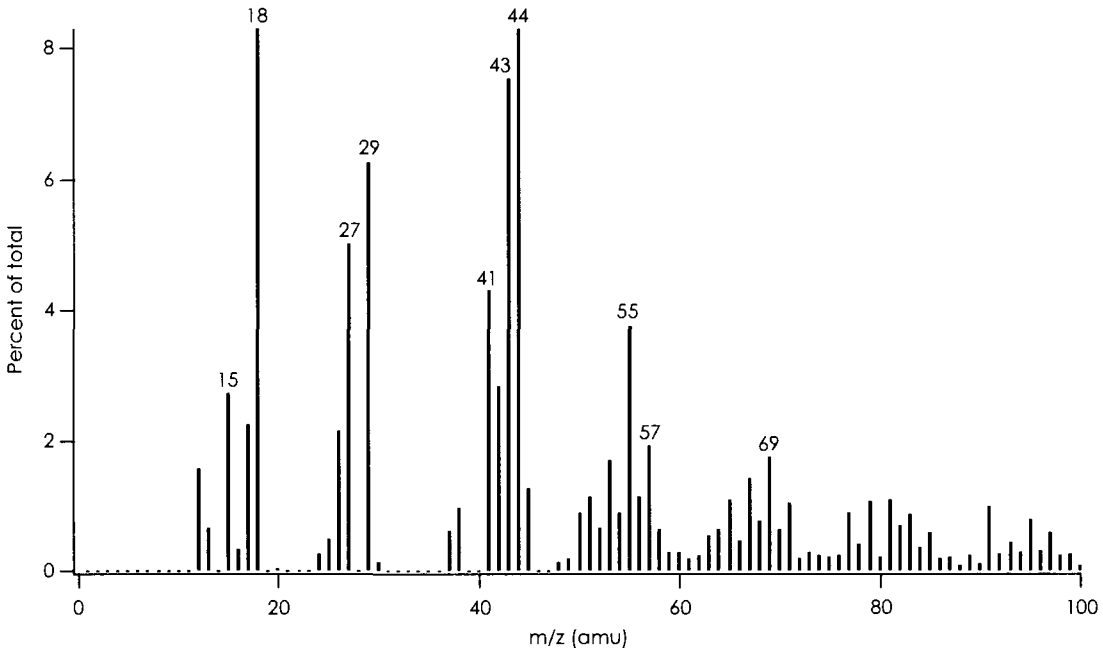

Figure 2 Average contribution of m/z ratios from 0-100 to the total organic signal over the entire campaign.

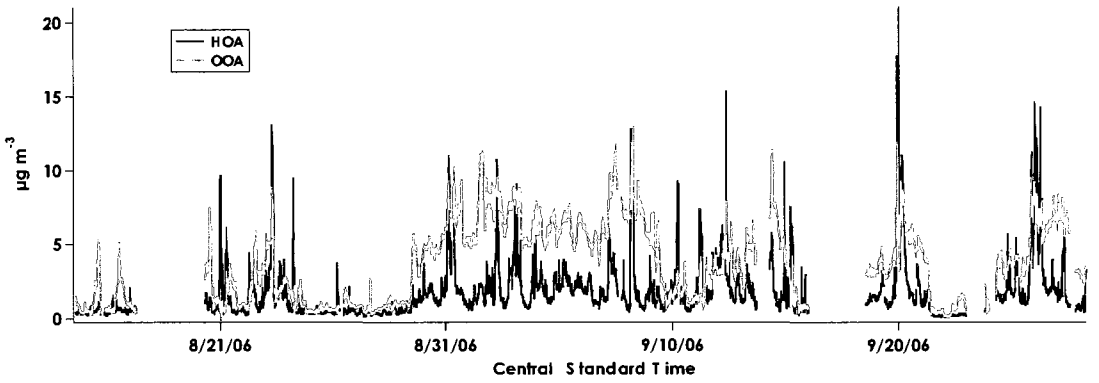

Figure 3 HOA and OOA traces for the entire TRAMP campaign.

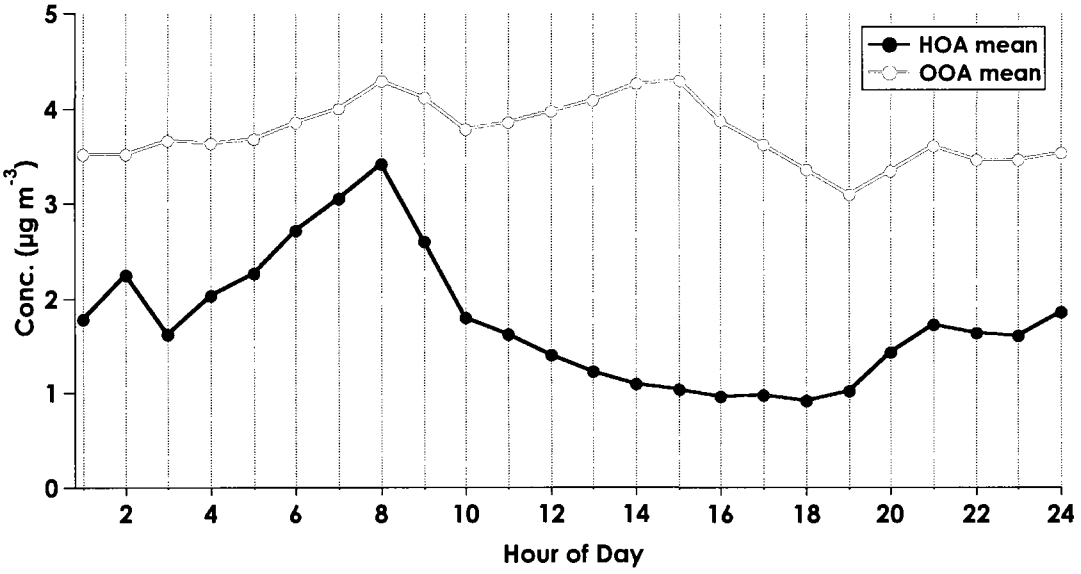

Figure 4 HOA and OOA average diurnal profiles.

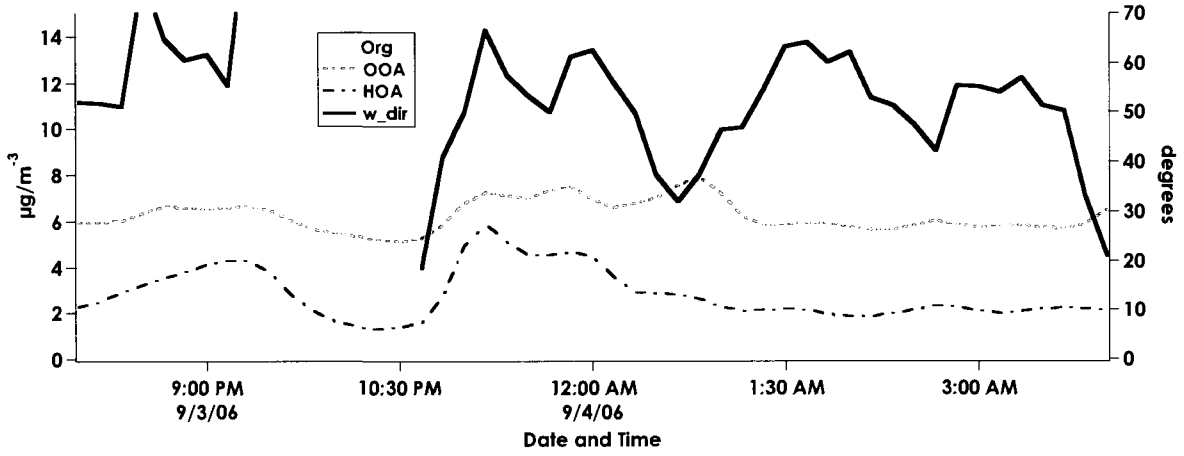

Figure 5 Typical event on 9/3 showing OA, OOA, and HOA mass concentrations and wind direction.

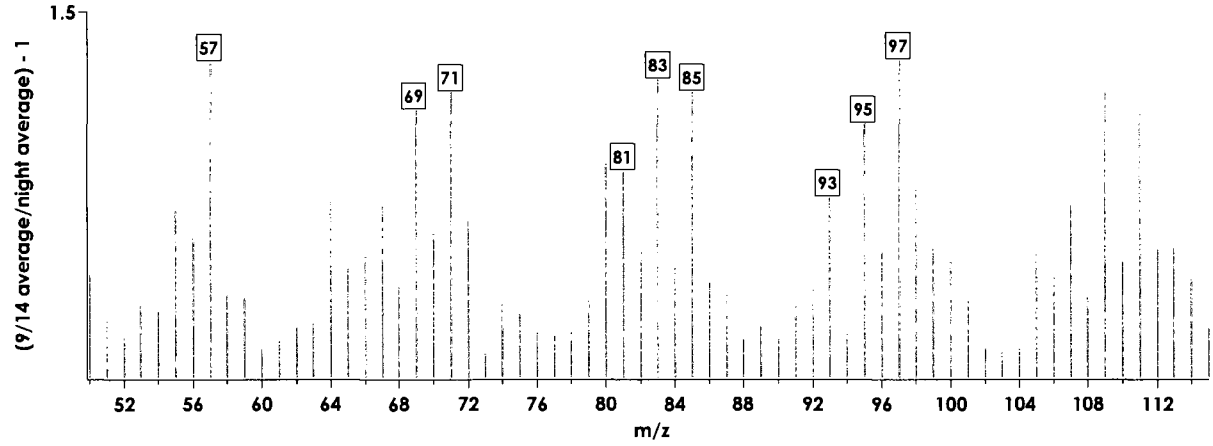

Figure 6 Comparison of the average organic spectrum during the 9/14 event to the campaign-average nighttime spectrum.

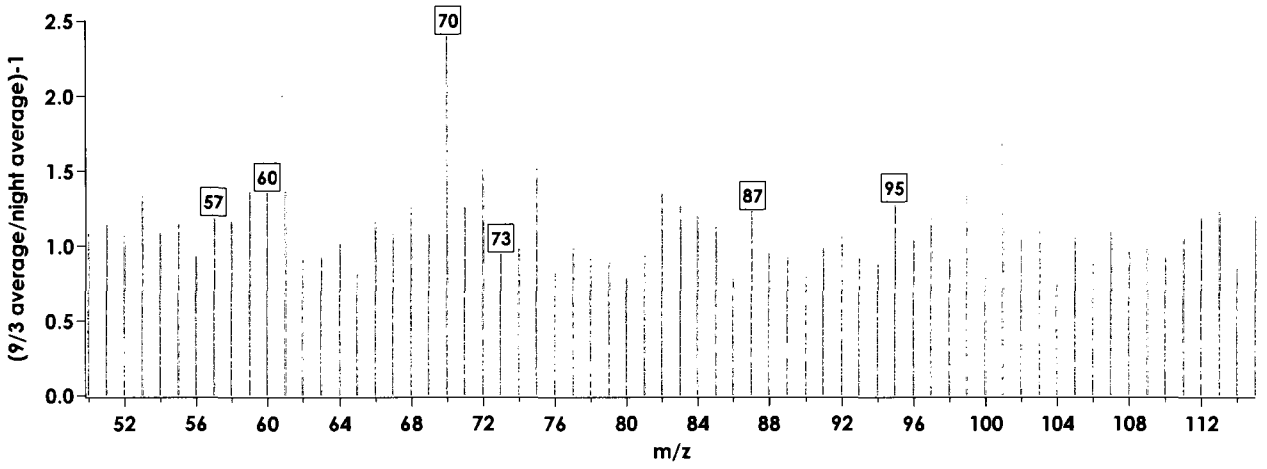

Figure 7 Comparison of the average spectrum during the 9/2 event with the campaign-average nighttime spectrum.

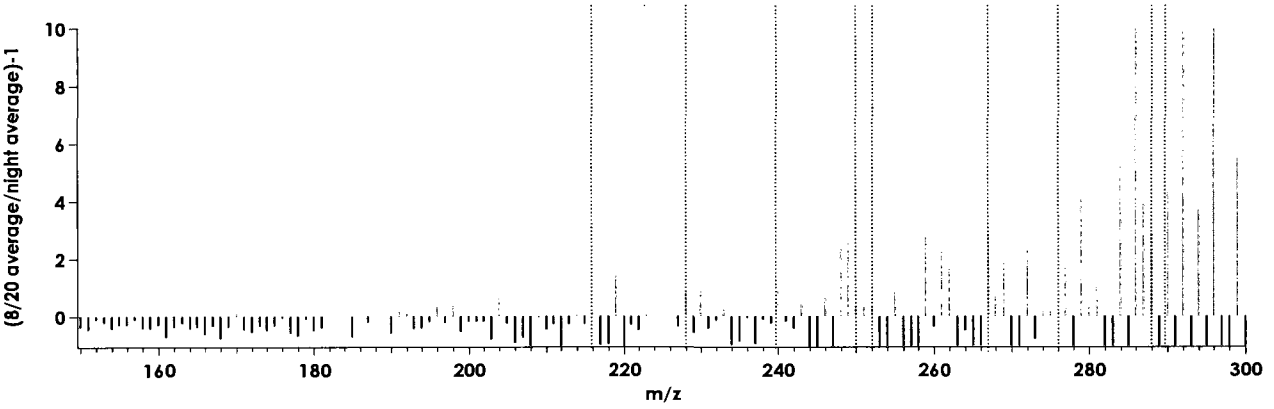

Figure 8 Ratio of the average spectrum during the 8/20 event to the average nighttime spectrum. Dashed lines represent m/z values representative of PAHs.

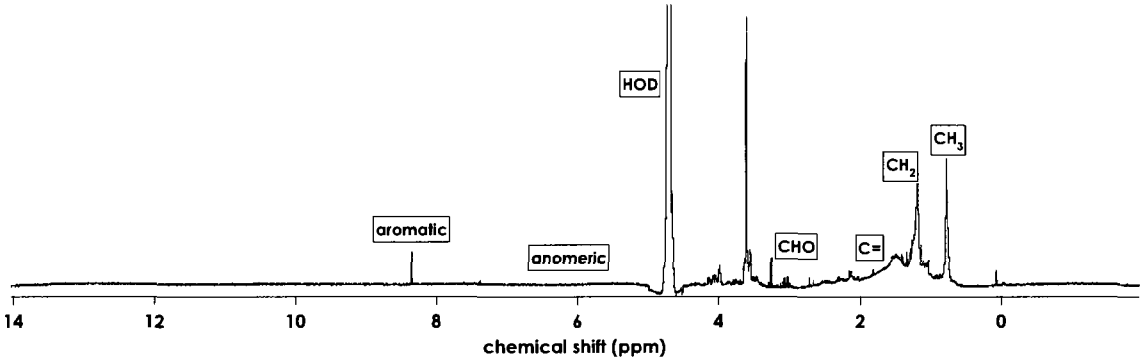

Figure 9 Average of all NMR spectra from the 29 samples from TRAMP. The average aromatic peak is skewed by the large contribution of one sample.

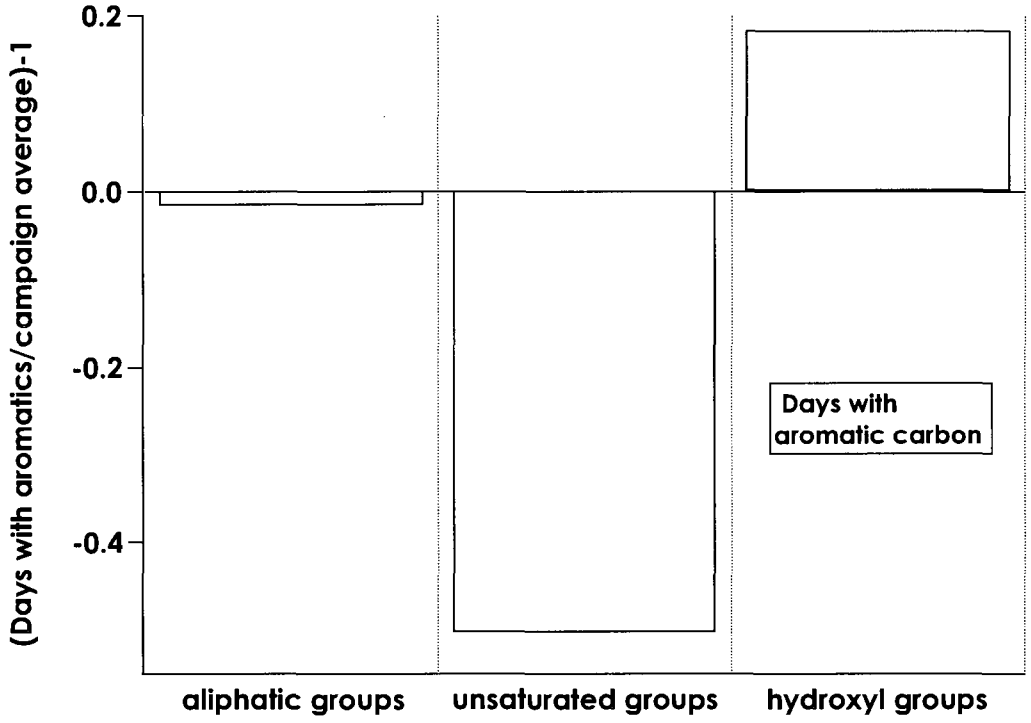

Figure 10 Comparison of average H-NMR signal on days with observed aromatic signal to the campaign average.

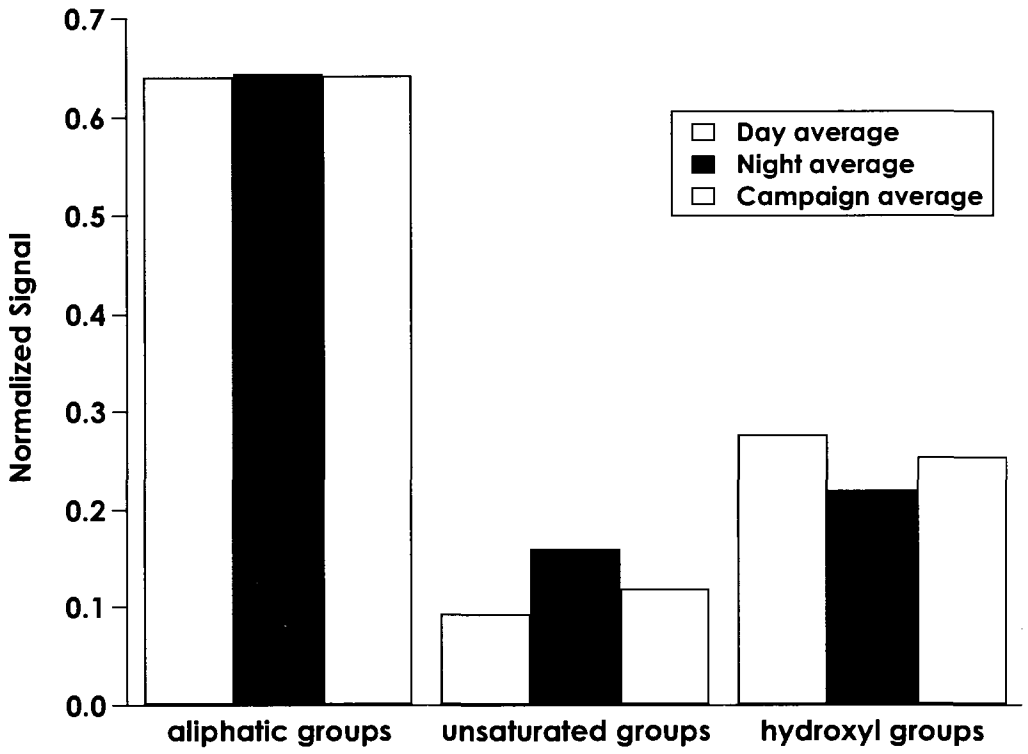

Figure 11 Average day, night, and campaign functional group budget for measured TRAMP aerosols. Anomeric and aromatic carbon are not shown due to negligible contributions.

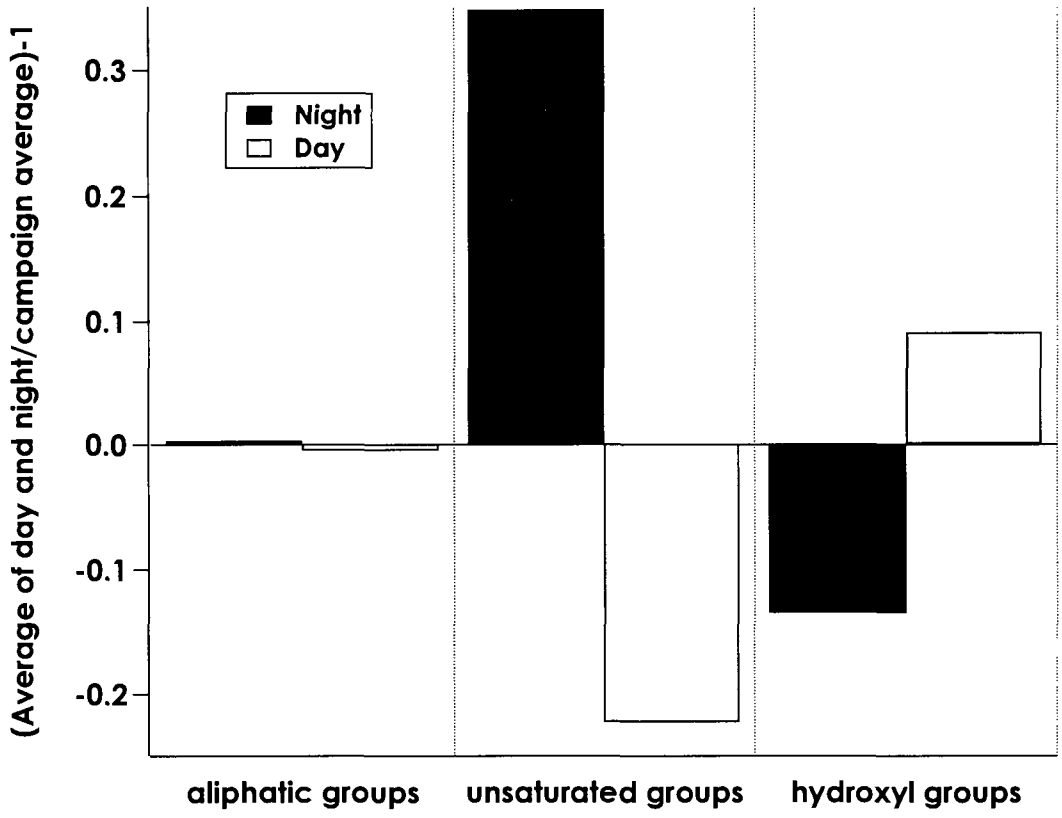

Figure 12 Diurnal enhancements of different functional groups during TRAMP. Enhancements (positive) and depletions (negative) are shown relative to total average signal. Anomeric and aromatic carbon are not shown due to negligible contributions.

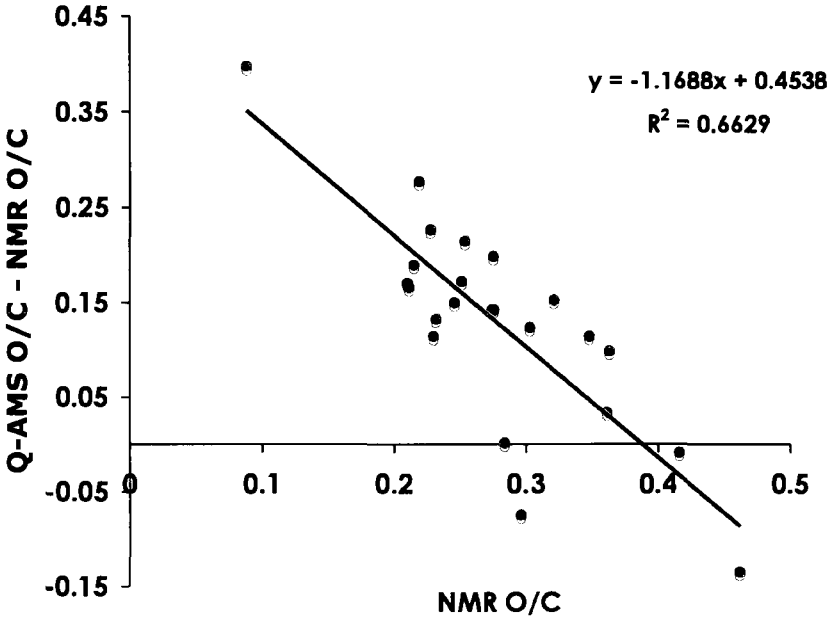

Figure 13 Correlation between the difference of the Q-AMS O/C ratios and the H-NMR O/C ratios and the H-NMR O/C

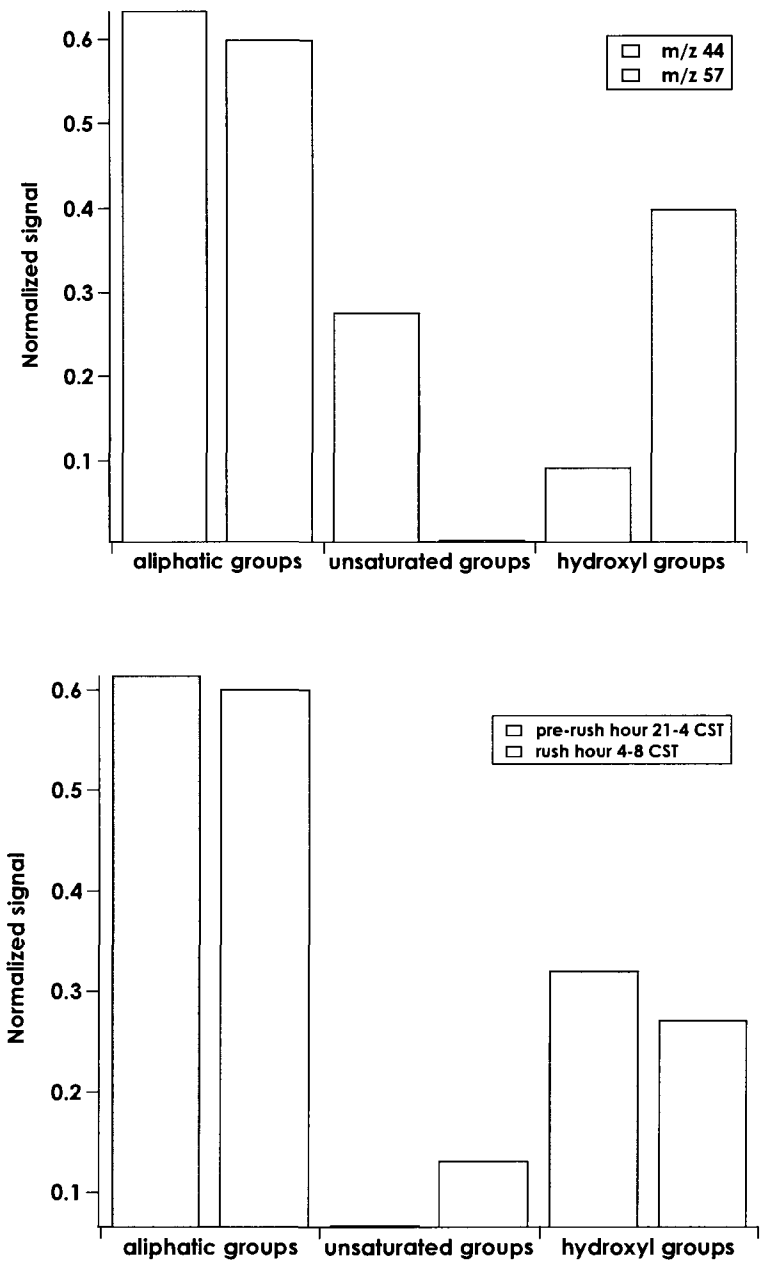

Figure 14 Normalized signal for the samples with the highest m/z 44 and 57 and for pre-rush hour and rush hour. Anomeric and aromatic carbon are again not displayed due to negligible contributions.

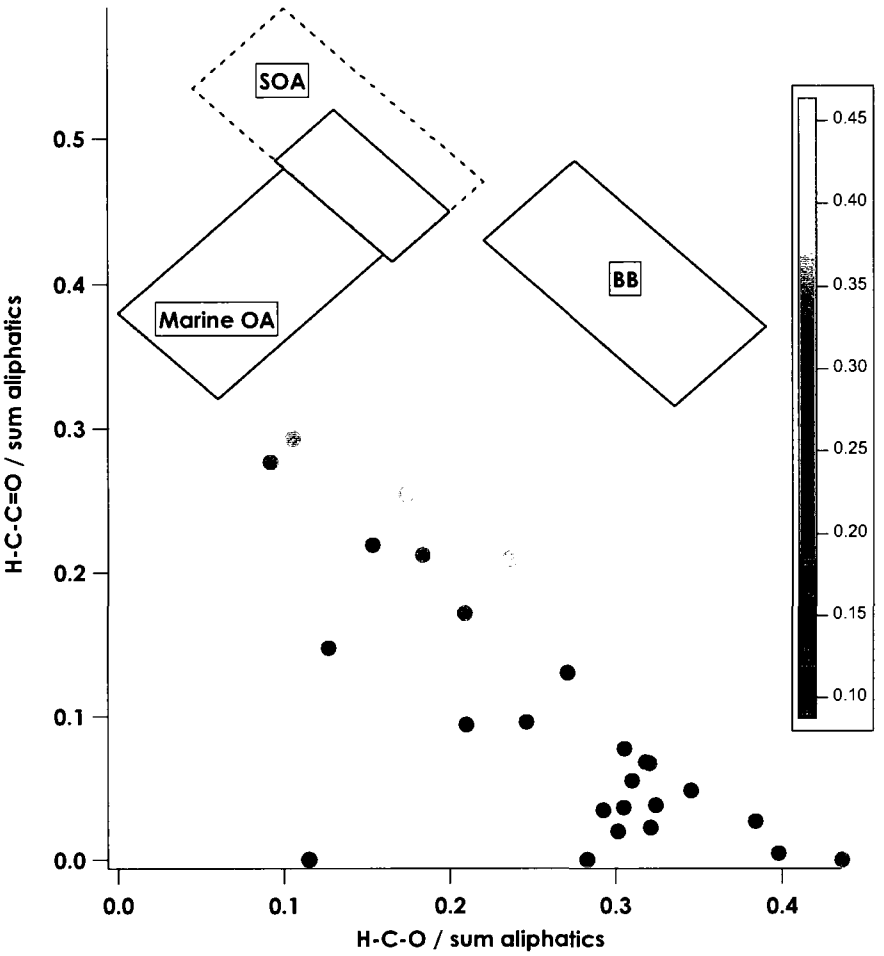

Figure 15 Functional group distributions for Houston, TX, during TRAMP based on the analysis of Decesari et. al (2007). Boxes represent previously established boundaries for marine OA, SOA, and biomass burning (BB). Points are colored by O/C ratios calculated using H-NMR functional groups.

Table 1 Q-AMS statistics for 10-minute averages for ammonium, nitrate, sulfate, organics, and chloride concentrations ($\mu g\ m^{-3}$) for entire campaign.

	NH4	NO3	SO4	Organics	Chloride	HOA	OOA
Average	0.92	0.38	4.08	5.46	0.10	1.74	3.74
Maximum	4.19	6.08	21.19	36.84	0.71	21.00	12.88
Minimum	0.03	0.03	0.23	0.45	0.03	0.05	0.01
Median	0.82	0.28	3.50	5.21	0.06	1.21	3.45
Std. Dev	0.52	0.45	2.62	4.00	0.09	1.90	2.63
5th percentile	0.29	0.05	0.96	0.78	0.03	0.22	0.45
25th percentile	0.55	0.11	2.16	1.83	0.04	0.57	1.09
75th percentile	1.20	0.49	5.54	7.68	0.11	2.09	5.70
95th percentile	1.91	1.16	9.04	12.60	0.31	5.35	8.15

Table 2 Correlation coefficients between HOA/OOA spectra and common POA/SOA spectra. Misc. includes r^2 coefficients between other measured time series and HOA/OOA time series.

		HOA (r^2)	OOA (r^2)
POA	Pittsburg HOA	**97**	
	Diesel Exhaust Aerosol	**97**	
	Lubricating Oil	**91**	
	Diesel Fuel	**77**	
SOA	Pittsburg OOA		**99**
	M-xylene + hv (SOA)		**94**
	Rural OA		**90**
	Fulvic Acid		**81**
MISC.	CO	**0.51**	0.23
	Sulfate	0.004	0.23
	Ammonium	0.04	0.33
	Nitrate	**0.45**	**0.41**

Table 3 List of OA nighttime events and characteristics

Start date/time	End date/time	Duration	Type of Event	Wind Direction	OOA/HOA ratio	O/C ratio	m/z 57 enhancement	m/z 69, 71, 81, 83, 85, 93, 95, and 97 enhancement	m/z 60, 73, 87, 100, and 114 enhancement	PAH enhancement
20-Aug 23:50	**21-Aug** 1:50	2 hours	Increasing HOA	130-160	Decreases	Very low 0.16	No	No	No	Yes 9 out of 14
29-Aug 21:10	**30-Aug** 1:50	3 hours 40 min	Gradual HOA	0-60	No significont change	Night average 0.39	Yes	Yes 85, 93, 95	Yes 60	Yes 11 out of 14
2-Sep 22:50	**3-Sep** 4:00	5 hours 10 min	Increasing HOA and OOA	0-35	Decreases	Night average 0.36	Yes	Yes 69, 71, 93, 95, 97	Yes 60, 73, 87	Yes 11 out of 14
3-Sep 22:40	**3-Sep** 1:10	2 hours 30 min	Increasing HOA	0-50	Decreases	Night average 0.36	Yes	Yes 83, 95, 97	Yes 60, 73, 87, 101	Yes 13 out of 14
14-Sep 23:30	**15-Sep** 1:20	1 hour 50 min	Increasing HOA	130-160	Variable due to rapid changes in HOA	Night average 0.37	Yes	Yes 69, 71, 81, 83, 93, 95	No	Yes 6 out of 14
19-Sep 22:00	**20-Sep** 1:40	3 hours 40 min	Increasing HOA ond OOA	0-50	Variable due to rapid changes in HOA	Low 0.28	Yes	Yes 69, 71, 83, 85, 95, 97	No	Yes 14 of out 14

Table 4 Correlation coefficients between OA mass and common VOCs during events

VOC	R^2
Acetylene	**0.68**
Benzene	**0.62**
1-3-Butadiene	0.36
Isobutene	0.32
Isoprene	0.06
Propane	0.33
Trichloroethylene	0.16
Toluene	**0.69**